

20th CIRP Conference on Modeling of Machining Operations

# Modelling the energy consumption of an industrial robot with different types of trajectory for machining tasks

Florian Delooz<sup>a,\*</sup>, Valentin Dambly<sup>b</sup>, François Ducobu<sup>b</sup>, Édouard Rivière-Lorphèvre<sup>b</sup>, Bryan Olivier<sup>a</sup>

<sup>a</sup>Department of Theoretical Mechanics, Dynamics and Vibrations, University of Mons, Place du Parc 20, 7000 Mons, Belgium

<sup>b</sup>Department of Machine Design and Production Engineering, University of Mons, Place du Parc 20, 7000 Mons, Belgium

\* Corresponding author. E-mail address: [florian.delooz@umons.ac.be](mailto:florian.delooz@umons.ac.be)

## Abstract

Industrial robots are being used more and more for machining operations, in particular due to their agility in the case of products with complex geometries, as well as their adaptability across various applications. For some years, as industries become more ecologically conscious, energy consumption (EC) during operations becomes an important consideration. This growing awareness motivates the need for models that monitor the EC of a robot during machining operations. Firstly, the robot multibody model used in the simulations will be completely described. The computational methodology used to calculate EC during these machining tasks will also be outlined, including a discussion of the motors model applied in the simulations. Then, to validate the established model, an initial simulation will be carried out using a simple general case, depicting a straight line trajectory, to demonstrate the effectiveness of the model used. Finally, other relevant simulation tests will be presented for distinct cases: a smooth and continuous machining trajectory with variations in the curve parameter and the followed axes. The results of these numerical tests provide insights into how different machining strategies impact EC, providing guidelines for optimizing robot operation in an environmentally conscious industrial context.

© 2025 The Authors. Published by Elsevier B.V.

This is an open access article under the CC BY-NC-ND license (<https://creativecommons.org/licenses/by-nc-nd/4.0>)

Peer-review under responsibility of the scientific committee of the 20th CIRP Conference on Modeling of Machining Operations in Mons

**Keywords:** Robotic Machining; Energy Consumption; Multibody Dynamics Simulation

## 1. Introduction

Industrial robots are used across many applications, including machining operations. The integration of robotics in this field presents numerous advantages, such as portability, adaptability among the different operations and to different machining geometries. Generally, trajectories required for machining are generated to achieve the desired accuracy and geometries of the parts, while also compensating for deflection due to the inherent flexibility of the robot [1, 2]. In these previous works, the optimisation was made from an operational point of view only, to reduce robot vibrations and deviations, which cause inaccuracies in machined parts.

Over the last few years, the industrial world, including both manufacturers and users, has developed a special concern for energy consumption (EC) in the various processes used, with methods that have sometimes been tried and tested for decades.

It is also necessary to pay close attention to this consideration in machining industry, so it is important to develop methods for measuring and controlling the EC in machining activities with industrial robots.

Building upon previous research on robot flexibility [1, 2] and in order to pursue trajectory optimisation, the incorporation of robot EC considerations will be explored to optimise machining articular trajectories for the same tool path.

EC monitoring for robots is already a highly investigated topic. Firstly, some studies are looking at the parameters that influence EC. Garcia et al. [3] identify these parameters at standstill, in motion and how joint friction is affected by some parameters as load, speed or temperature. Guerra-Zubiaga et al. [4] study the influence of speed, acceleration, load and temperature through experiments and conclude that nearly 95 % of EC for the robot studied is due to linear speed and acceleration. Liu et al. [5] work on the EC modelling by using software-simulated power data to perform parameter identification, since some parameters, such as inertia or friction, of industrial robots are unknown to users.

**Nomenclature**

$\vec{F}$	Vector gathering the contribution of external forces
$\vec{h}$	Vector gathering the centrifugal and Coriolis contributions
$i_{m,i}$	Current for motor at joint $i$ [A]
$k_i$	Gear ratio at joint $i$ ( $> 1$ )
$K_{t,i}$	Torque constant for motor at joint $i$ [(N · m)/A]
$K_{v,i}$	Back electromotive force constant for motor at $i$ [V · s]
$M$	Mass matrix
$P_{m,i}$	Electrical power of motor $i$ [W]
$\vec{q}_m$	Vector of degrees of freedom representing the instantaneous position of the motor shaft seen from the motor side
$\vec{q}_j$	Vector of degrees of freedom representing the instantaneous position of the motor shaft seen from the joint side
$R_{a,i}$	Armature resistance for motor at $i$ [ $\Omega$ ]
$u_{m,i}$	Voltage for motor at joint $i$ [V]
$\vec{\tau}_m$	Vector of actuator torques

Other works seek to develop optimisation methods. For example, Gadaleta et al. [6] develop a simulation tool, with respect to the current robot offline programming tools, to compute energy-optimal parameters (based on velocity and acceleration limits) settable by the robot control codes. Matlab software is also used to produce configurations that reduce EC. For each task, Mohammed et al. [7] solve the inverse kinematics of the robot to obtain a set of potential joint configurations, compute EC for each of these configurations and optimise by selecting the configuration with the lowest consumption. Pellicciari et al. [8] use time scaling of pre-defined joint trajectories and preserve technological constraints, where EC is modeled as a function of a fifth-order polynomial equation to minimise. To optimise EC, Li et al. [9] focus on the trajectory optimisation problem and implement the sequential quadratic programming (SQP) method to solve it and obtain smooth movement. Some research uses neural network to predict and optimise EC [10, 11].

The estimation of EC will also depend on the way the robot is modelled and how precise this modelling is. The Matlab Robotics toolbox is regularly used to build robot model [9, 12], while Mohammed et al. [7] implement their developed modules in Matlab software. Othman et al. [13] use SolidWorks software to perform a geometrical model, which is modified into a Simulink model to perform simulation. Paryanto et al. [14] use CATIA Systems Dynamic Behavior Modeling, based on open source Modelica language, to create their digital model.

The aim of this article is to propose a sufficiently accurate digital shadow of the Stäubli TX200 industrial robot. It enables simulations on different types of trajectory used in machining operations in order to predict the EC of the robotic arm during these operations.

This work is based on recent research [1, 15], that have resulted in the development of the static and dynamic trajectory

compensation method, divided as: compensation of the robot structural deflections induced by gravity and compensation for deviations caused by cutting forces.

This paper is organized as follows: in Section 2, the multi-body modelling of the robot Stäubli TX200, used as an example in this study, will be presented. Consideration will be given to the flexibility of the robot, as well as the modelling of motors and the calculation of power consumption. In order to validate this model, an initial simple trajectory will be simulated in Section 3. Other more complex trajectories will be simulated and their results discussed in Section 4. The final comments and outlook are addressed in the [Conclusions and perspectives](#) section.

**2. Flexible multibody dynamic model**

A complete model of the 6-axis industrial robot studied in this paper has been developed [2, 15] and improved [1] to allow numerical simulations. The graphical representation of the robot can be seen in Figure 1. The generalised equations (1) of the robot are symbolically written, where  $M(\vec{q})$  contains inertial terms,  $\vec{h}(\vec{q}, \dot{\vec{q}})$  contains centrifugal and Coriolis terms,  $\vec{F}(\vec{q}, \dot{\vec{q}}, t)$  contains external forces:

$$M(\vec{q}) \cdot \ddot{\vec{q}} + \vec{h}(\vec{q}, \dot{\vec{q}}) = \vec{F}(\vec{q}, \dot{\vec{q}}, t) \quad (1)$$

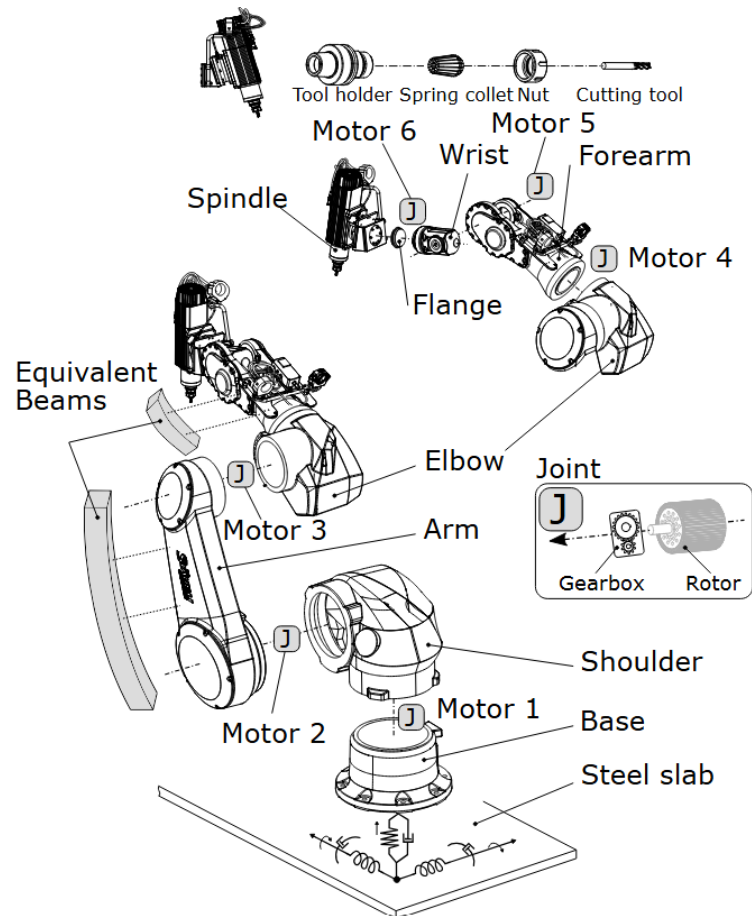


Fig. 1: Global representation of Stäubli TX200 [1]

Indeed, this robot model is described by 40 degrees of freedom, including the 6 actuated degrees  $\vec{q}_a$  of the axes and 34 unactuated degrees  $\vec{q}_u$  added to model some specific behaviours.

First of all, inherent robot flexibility exists and is mainly located at:

- Articulations level [2]: modelling approach based on tri-axial flexibility, such that spring-damper pairs are considered in each direction of the joint local frame ( $3 \times 6 \vec{q}_u$ )
- Structural level: on arm and forearm, and their flexibility are modelled with the corotational formulation in minimal coordinates, which means that the robot body can be approximated as flexible beams with nodes placed at the extremities, whose motion allows to represent the motion of the flexible body ( $6 \times 2 \vec{q}_u$ )

Three  $\vec{q}_u$  are added between the steel slab and the robot base to model the clamping of the base on the steel slab, which is a source of flexibility. A Dynamic Vibration Absorber (DVA) allows to limit the effect of a natural frequency of the robot ( $1 \vec{q}_u$ ).

Motion and forces are modelled and computed thanks to specific in-house developed simulators as EasyDyn [16] for flexible multibody dynamics. The developments presented in this paper can be coupled with cutting dynamics and efforts modelling with Dystamill [17], with 3D cutting extension [18], to add this element to the consumption estimate. In the case of these simulations, no machining is implemented.

### 2.1. Trajectory generation

In this part, the way to generate the desired trajectories to apply to the robot, developed in [1], is briefly presented.

Firstly, as depicted in Figure 2, the path is discretised as a point cloud based on the G-code commands. Then, for complex motion, the G-code consists of a series of lines. A file is generated containing information on the point  $i$  such as the curvilinear abscissa  $s_i$  and its derivatives, time  $t_i$ , position  $\vec{e}_i$  and its derivatives, tangent to the path  $\frac{d\vec{e}_i}{ds}$ , quaternion for spindle orientation and rotational speed  $\vec{\omega}_i$ . To perform the interpolation, the normalized curvilinear abscissa  $u$  is used, and it is obtained from  $s$  by a root finding method. Among the  $n$  points in the list, an adequate number  $n_{nodes}$  is selected to perform the interpolation between them and reproduce the desired path, as depicted on the right plot of Figure 2. The nodes distribution along the path is a studied factor [1], and an optimisation is made on their number such that parameters  $\frac{ds}{du}$  and  $\frac{d^2s}{du^2}$  are best suited to the desired path. The selected method to interpolate between nodes is Hermite splines of 5<sup>th</sup> order, to locate nodes on the path and to generate a trajectory with continuity class  $C_1$  on acceleration [1].

The speed profile associated with the path is also considered. Linear segments with parabolic blending (*ls pb*) allow to smooth trajectory variations. In this case, a Hermite spline approximation is preferred to obtain smoother velocity variations [1].

The generated trajectory can then be applied to the robot model to perform the simulation. In the previous work [1], the deviations due to robot flexibility and cutting forces are compensated by updating the path.

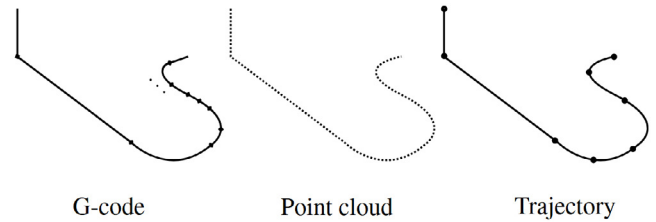


Fig. 2: Interpolation nodes obtained from G-code [1]

### 2.2. Actuator modelling

The actuators still need to be modelled for each joint and allow them to move so that the robot achieves the desired trajectory. The actuators of the studied robot are electric servomotors. As a first approximation, they are modelled as brushless DC motors (Figure 3).

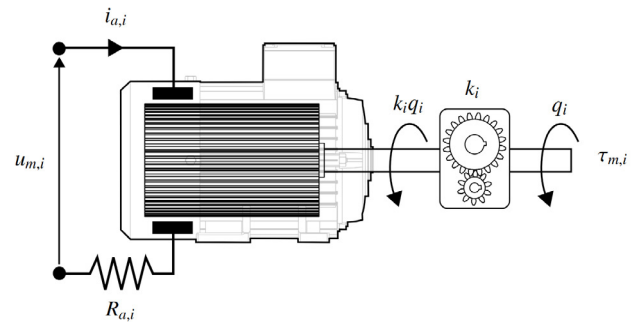


Fig. 3: Model of a DC motor [19]

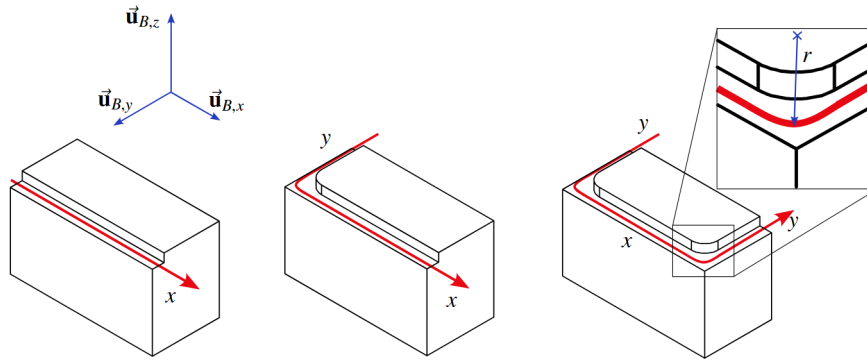
For each joint  $i$  ( $i = 1, \dots, 6$ ), the relation (2) between the torque generated by the motor  $i$  and the current is:

$$\tau_{m,i} = K_{t,i} \cdot i_{m,i} \quad (2)$$

With the second Kirchhoff's law applied to the DC motor and the assumption that inductance effects can be neglected due to the faster rate of electrical phenomena compared to mechanical effects, motor torque equation (3) is such that:

$$\tau_{m,i} = \frac{K_{t,i}}{R_{a,i}} (u_{m,i} - K_{v,i} \dot{q}_{m,i}) \quad (3)$$

In reality, the robot's electric actuators are AC permanent magnet synchronous motors. Both share the same architecture, the advantage of making this modification lies in the fact that the control strategy to be implemented in the model is less complex [19]. Indeed, large robot movements are being tested here, so the time constant for electrical phenomena is relatively small compared with those for mechanical effects. The hypothesis is therefore that the influence of these electrical phenomena is limited, which makes it possible to simplify the motor architecture.


 Fig. 4: Machining trajectories  $x$ ,  $y2x$  and  $y2x2y$ 

For the control, the assumption of centralised inverse dynamic control is made, based on the equations of the rigid robot because no sensors are measuring robot deflection [1].

### 2.3. Energy consumption calculation

The various equations implemented will be used to calculate energy consumption and the parameter selected for this is electrical power. Therefore, it is necessary to have the voltage and current equations (4). Note that the degrees of freedom managed during the simulation are those seen from the joint side  $\vec{q}_j$ , and they are linked with  $\vec{q}_m$  by the gear ratio  $k_i$  (for the  $i$ -th joint).

$$\begin{aligned} u_{m,i} &= R_{a,i} \cdot i_{m,i} + K_{v,i} \cdot \dot{q}_{m,i} \\ i_{m,i} &= \frac{\tau_{m,i}}{K_{t,i}} \\ P_{m,i} &= u_{m,i} \cdot i_{m,i} \end{aligned} \quad (4)$$

### 3. Case of a simple trajectory

In order to test the model of the robot created, an initial simple simulation will be carried out. It allows to compute EC in a simple case to verify whether the order of magnitude of the values obtained is consistent. The selected machining trajectory for this test corresponds to a straight line trajectory along the  $x$  axis (Figure 4, where the workpiece is represented to facilitate understanding trajectories, but there is no actual machining in the simulations). The aim here is to quantify the consumption of the robot just for the positioning task.

The evolution of the power of the Stäubli motors can be seen in Figure 5. It can be seen that the power rating of the first and sixth motors is almost zero. Indeed, the first motor and the sixth motor correspond respectively to the base/shoulder motor and to the wrist/flange (Figure 1). These two axes are hardly used at all in the movement performed, as it can be seen from the position of the robot in relation to the workpiece in Figure 6.

The motor with the highest power is the second motor, corresponding to the shoulder. This power starts around 2000 W, increases to stabilise around 2600 W. It corresponds to the way this joint works. The robot shoulder holds the significant overhang, and this overhang increases during the machining trajectory.

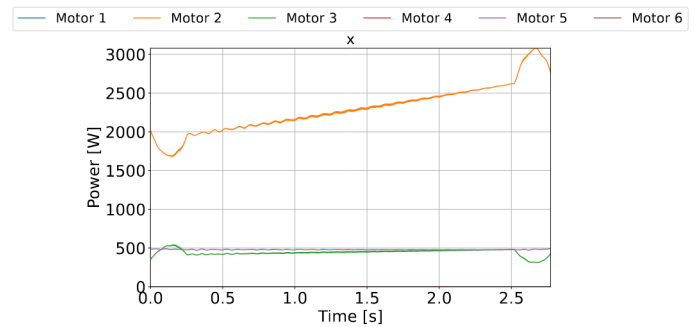
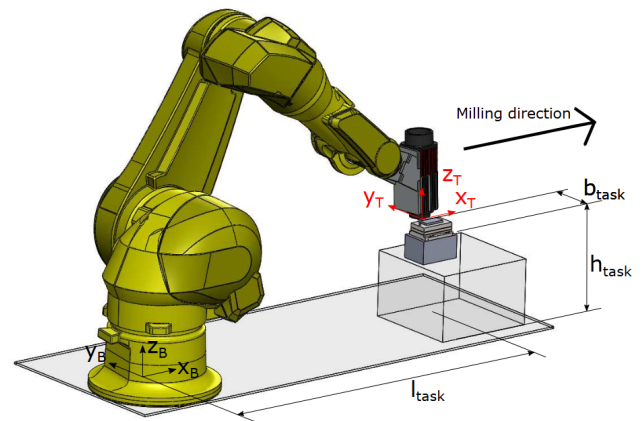

 Fig. 5: Power consumption of the Stäubli motors during  $x$  trajectory


Fig. 6: Robot configuration for simulated machining paths [1]

The power level of the fifth motor (at wrist) is almost constant at 500 W while the power level of the third motor (at elbow) remains between 400 and 500 W. This is explained by the role of these two axes in the movement. They allow the spindle to be straightened and reoriented downwards (to guarantee the correct orientation of the end-effector) as the arm moves away from the base (along the  $x$  axis) with the evolution of the shoulder axis. The spindle is straightened constantly during movement, since everything is done at a constant speed, which explains why the power consumed is also more or less constant, the change in power associated with the movement seems slight.

The power of the fourth motor (at forearm) is also almost zero. This axis is active when there is a change from the  $x$  direction to the  $y$  direction, given the orientation of the robot with respect to the workpiece (Figure 6). It is not the case in this simulated trajectory.

The developed model can be used to deduce values and gives coherent developments, but validation on an energy point of view (with measures on robot) is planned in further work.

#### 4. Simulation tests and results

Once the model is tested with the simple trajectory according to  $x$ , other trajectories can be tested. Two trajectories are selected: a trajectory along the  $y$  axis and then  $x$  axis, called  $y2x$  (Figure 4), and a trajectory along  $y$ ,  $x$  and then  $y$  axis, called  $y2x2y$  (Figure 4).

For each of these trajectories, two cases are considered. To link the two or three linear paths, a rounded corner is included. The radius of this corner can be modified, to make the change of direction smoother. Two radius values are tested:  $r = 8$  mm and  $r = 12$  mm.

The evolution of the power of the Stäubli robot motors for these four trajectories can be viewed in Figure 7. For the reasons explained in the previous Section 3, the powers of the first and sixth motors are not shown so as not to overload the graph. It can be seen that the power of the motor at the base (in blue on the graphics) has a development similar to that already described in Section 3. Indeed, for  $y2x$  path, the consumption is initially constant, which corresponds to movement along the  $y$  axis, which is parallel to the shoulder axis, so the range does not vary significantly. Then power increases, which corresponds to the movement described along the  $x$  axis in Section 3. For  $y2x2y$  path, after the two developments described above, there is still a constant power level, which corresponds to the end of the path along the  $y$  axis. For the third and fifth motors, the evolution is still the same than for Section 3, to maintain correct spindle orientation. Finally, the power consumed by the fourth motor remains zero except during the change of direction between  $x$  and  $y$ , since this joint is mobilised.

EC can be deduced from power by calculating the integral of the latter as a function of time. The results are presented in the Table 1, for each trajectory and each motor. It can be observed that the EC of the first and sixth motors are null for the five performed trajectories. Two main observations can be made from these data. Firstly, for the same trajectory, a larger corner radius  $r$  reduces the EC of each joint. This is to be expected, as it makes the change of trajectory smoother. Secondly, for the trajectories tested, the robot's EC is mainly due to the first three joints of the robot, i.e. the structural joints: base, shoulder and elbow (see the first series in the Table 1). The other three joints (forearm, wrist and flange) consume less energy. The EC of the first three joints is 85.09 %, 84.35 %, 84.41 %, 84.36 % and 84.45 %, respectively for the five trajectories tested. EC is therefore due to the placement of the forearm rather than the orientation of the tool.

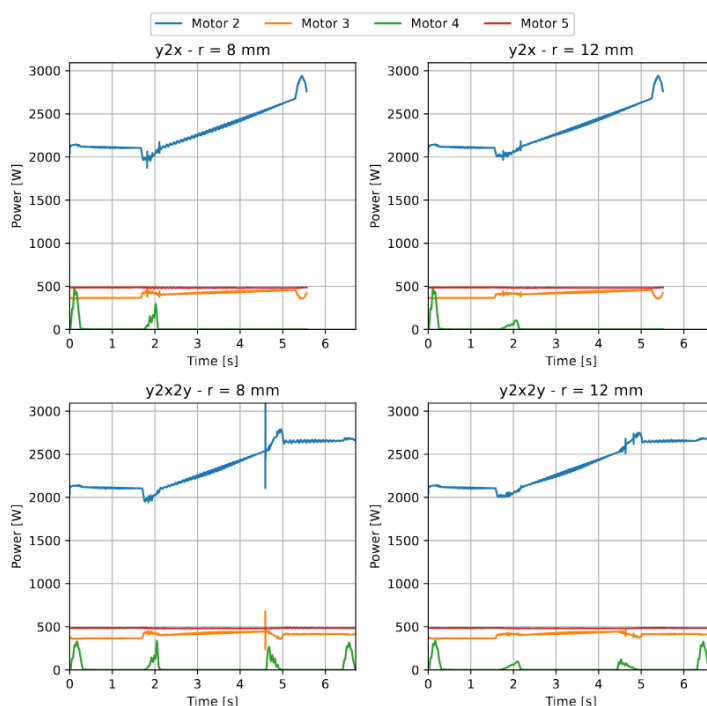


Fig. 7: Power consumption of the Stäubli motors during four machining trajectories

Table 1: Energy consumed by motors for the five different simulated trajectories

Trajectory	Motor 1 [J]	Motor 2 [J]	Motor 3 [J]
$x$	0.00	6363.75	1228.06
$y2x$ ( $r = 8$ mm)	1.93	12773.04	2271.35
$y2x$ ( $r = 12$ mm)	1.67	12659.49	2251.31
$y2x2y$ ( $r = 8$ mm)	3.39	15801.13	2723.71
$y2x2y$ ( $r = 12$ mm)	2.85	15544.40	2681.25

Trajectory	Motor 4 [J]	Motor 5 [J]	Motor 6 [J]
$x$	0.61	1329.97	0.03
$y2x$ ( $r = 8$ mm)	103.06	2689.52	0.10
$y2x$ ( $r = 12$ mm)	90.16	2663.20	0.10
$y2x2y$ ( $r = 8$ mm)	183.20	3251.40	0.08
$y2x2y$ ( $r = 12$ mm)	157.39	3198.79	0.08

Trajectory	Total [J]	Total/trajectory [J/mm]
$x$	8922.42	63.73
$y2x$ ( $r = 8$ mm)	17839.00	101.03
$y2x$ ( $r = 12$ mm)	17665.93	101.03
$y2x2y$ ( $r = 8$ mm)	21962.91	103.05
$y2x2y$ ( $r = 12$ mm)	21584.76	102.93

## 5. Conclusions and perspectives

In this paper, a robot multibody model is presented to perform machining trajectories simulation in order to predict EC. First, a brief review of the scientific literature is conducted. It mainly shows that the robot's power consumption is due to the speed and acceleration setpoints. It also presents techniques to optimise the EC of robots and shows that the use of commercial software to build the robot model is widespread.

The 6-axis industrial robot model takes into account flexibility at different levels thanks to unactuated degrees, added to the actuated degrees located at the joints. Trajectories are performed by interpolation between nodes with Hermite splines of 5th order, and smooth trajectory variations are considered. To allow the robot to move, brushless DC motors are modelled and their electric equations used to calculate power and energy consumption during the path simulations.

A first simple simulation, representing a motion along  $x$  axis, is performed to validate the built model. The evolution of power for each joint is consistent with their use for this path. Trajectories along  $x$  and  $y$  axes are then tested, for different values of radius corner between linear paths. They confirm the initial observations, as well as demonstrating the benefits of a larger radius when changing direction, and the preponderance of EC by the robot's three joints (around 85 % of total energy consumed). Other types of trajectory, with different parameter values or for more complex movements, will be tested in further research. The change in the radius of curvature of the trajectory has an influence on accelerations imposed on the end-effector, that are linked to the robot EC.

Subsequent perspectives for continuing the study have already been identified. EC experimental measurements are to be taken on the Stäubli TX200 robot, in order to identify potential differences between the results of the simulated model and those of the real model, enabling the digital shadow to be improved, in order to establish a predictive model of the industrial robot EC. These measurements under real conditions would also make it possible to compare the power consumption of the robot and that of the spindle for machining operations and to see the relative importance of these consumptions. With the same purpose, the comparison with the total consumption of the electrical cabinet over a day (including idle time) will be performed. In the established model, an acceptable simplifying assumption has been made concerning the modelling of the motors. In the future, it will be interesting to adapt this model to match the motor architecture as closely as possible.

## References

- [1] Valentin Dambly. *Robotic Machining: Tool Trajectories Adaptation to Correct the Dynamic and Static Inaccuracies*. PhD thesis, University of Mons, September 2023.
- [2] Hoai Nam Huynh, Hamed Assadi, Valentin Dambly, Edouard Rivière-Lorphèvre, and Olivier Verlinden. Direct method for updating flexible multibody systems applied to a milling robot. *Robotics and Computer-Integrated Manufacturing*, 68:102049, April 2021. doi: [10.1016/j.rcim.2020.102049](https://doi.org/10.1016/j.rcim.2020.102049).
- [3] Raphael Rustici Garcia, André Carvalho Bittencourt, and Emilia Villani. Relevant factors for the energy consumption of industrial robots. *Journal of the Brazilian Society of Mechanical Sciences and Engineering*, 40(9):464, September 2018. doi: [10.1007/s40430-018-1376-1](https://doi.org/10.1007/s40430-018-1376-1).
- [4] David A. Guerra-Zubiaga and Kimberly Y. Luong. Energy consumption parameter analysis of industrial robots using design of experiment methodology. *International Journal of Sustainable Engineering*, 14(5):996–1005, September 2021. doi: [10.1080/19397038.2020.1805040](https://doi.org/10.1080/19397038.2020.1805040).
- [5] Aiming Liu, Huan Liu, Bitao Yao, Wenjun Xu, and Ming Yang. Energy consumption modeling of industrial robot based on simulated power data and parameter identification. *Advances in Mechanical Engineering*, 10(5):1687814018773852, May 2018. doi: [10.1177/1687814018773852](https://doi.org/10.1177/1687814018773852).
- [6] Michele Gadaleta, Marcello Pellicciari, and Giovanni Berselli. Optimization of the energy consumption of industrial robots for automatic code generation. *Robotics and Computer-Integrated Manufacturing*, 57:452–464, June 2019. doi: [10.1016/j.rcim.2018.12.020](https://doi.org/10.1016/j.rcim.2018.12.020).
- [7] Abdullah Mohammed, Bernard Schmidt, Lihui Wang, and Liang Gao. Minimizing Energy Consumption for Robot Arm Movement. *Procedia CIRP*, 25:400–405, January 2014. doi: [10.1016/j.procir.2014.10.055](https://doi.org/10.1016/j.procir.2014.10.055).
- [8] M. Pellicciari, G. Berselli, F. Leali, and A. Vergnano. A method for reducing the energy consumption of pick-and-place industrial robots. *Mechatronics*, 23(3):326–334, April 2013. doi: [10.1016/j.mechatronics.2013.01.013](https://doi.org/10.1016/j.mechatronics.2013.01.013).
- [9] Yumeng Li, Zhengdao Wang, Hui Yang, Hua Zhang, and Yikun Wei. Energy-Optimal Planning of Robot Trajectory Based on Dynamics. *Arabian Journal for Science and Engineering*, 48(3):3523–3536, March 2023. doi: [10.1007/s13369-022-07185-7](https://doi.org/10.1007/s13369-022-07185-7).
- [10] Pei Jiang, Zuoxue Wang, Xiaobin Li, Xi Vincent Wang, Bodong Yang, and Jiajun Zheng. Energy consumption prediction and optimization of industrial robots based on LSTM. *Journal of Manufacturing Systems*, 70:137–148, October 2023. doi: [10.1016/j.jmsy.2023.07.009](https://doi.org/10.1016/j.jmsy.2023.07.009).
- [11] Mingyang Zhang and Jihong Yan. A data-driven method for optimizing the energy consumption of industrial robots. *Journal of Cleaner Production*, 285:124862, February 2021. doi: [10.1016/j.jclepro.2020.124862](https://doi.org/10.1016/j.jclepro.2020.124862).
- [12] Koen Paes, Wim Dewulf, Karel Vander Elst, Karel Kellens, and Peter Slaets. Energy Efficient Trajectories for an Industrial ABB Robot. *Procedia CIRP*, 15:105–110, January 2014. doi: [10.1016/j.procir.2014.06.043](https://doi.org/10.1016/j.procir.2014.06.043).
- [13] Akeel Othman, Květoslav Belda, and Pavel Burget. Physical modelling of energy consumption of industrial articulated robots. In *2015 15th International Conference on Control, Automation and Systems (ICCAS)*, pages 784–789, October 2015. doi: [10.1109/ICCAS.2015.7364727](https://doi.org/10.1109/ICCAS.2015.7364727).
- [14] Paryanto, Matthias Brossog, Martin Bornschlegel, and Jörg Franke. Reducing the energy consumption of industrial robots in manufacturing systems. *The International Journal of Advanced Manufacturing Technology*, 78(5):1315–1328, May 2015. doi: [10.1007/s00170-014-6737-z](https://doi.org/10.1007/s00170-014-6737-z).
- [15] Hoai Nam Huynh, Hamed Assadi, Edouard Rivière-Lorphèvre, Olivier Verlinden, and Keivan Ahmadi. Modelling the dynamics of industrial robots for milling operations. *Robotics and Computer-Integrated Manufacturing*, 61:101852, February 2020. doi: [10.1016/j.rcim.2019.101852](https://doi.org/10.1016/j.rcim.2019.101852).
- [16] Olivier Verlinden, Lassaad Ben Fékik, and Georges Kouroussis. Symbolic generation of the kinematics of multibody systems in EasyDyn: From MuPAD to Xcas/Giac. *Theoretical and Applied Mechanics Letters*, 3(1):013012, January 2013. doi: [10.1063/2.13013012](https://doi.org/10.1063/2.13013012).
- [17] Hoai Nam Huynh, Edouard Rivière-Lorphèvre, François Ducobu, Abdullah Ozcan, and Olivier Verlinden. Dystamill: A framework dedicated to the dynamic simulation of milling operations for stability assessment. *The International Journal of Advanced Manufacturing Technology*, 98(5):2109–2126, September 2018. doi: [10.1007/s00170-018-2357-3](https://doi.org/10.1007/s00170-018-2357-3).
- [18] Valentin Dambly, Édouard Rivière-Lorphèvre, François Ducobu, and Olivier Verlinden. Tri-dexel-based cutter-workpiece engagement: Computation and validation for virtual machining operations. *The International Journal of Advanced Manufacturing Technology*, 131(2):623–635, March 2024. doi: [10.1007/s00170-023-10950-z](https://doi.org/10.1007/s00170-023-10950-z).
- [19] Hoai Nam Huynh. *Robotic Machining: Development and Validation of a Numerical Model of Robotic Milling to Optimise the Cutting Parameters*. PhD thesis, University of Mons, September 2019.